Science of the Total Environment 651 (2019) 2874–2885

Contents lists available at ScienceDirect

Science of the Total Environment

journal homepage: www.elsevier.com/locate/scitotenv

Soil and climate differently impact NDVI patterns according to the season and the stand type

C. Piedallu [a,*], V. Chéret [b], J.P. Denux [b], V. Perez [a], J.S. Azcona [a], I. Seynave [a,b], J.C. Gégout [a]

[a] Université de Lorraine, AgroParisTech, Inra, Silva, F-54000 Nancy, AgroParisTech, 14 rue Girardet, F-54042 Nancy Cedex, France
[b] Dynafor, Université de Toulouse, INRA, INPT, INPT - EI PURPAN, Castanet-Tolosan, France, École d'Ingénieurs de PURPAN, 75 voie du TOEC, BP57611, 31076 Toulouse Cedex 3, France

HIGHLIGHTS

- NDVI indices were modeled for different seasons using 20 environmental predictors.
- In spring, low temperatures, nitrogen availability, and pH limit greenness.
- In summer, low soil water reserve and high temperatures are the main constraints.
- The factors limiting vegetation dynamics vary according to the stands type.
- Our findings are helpful to adapt our forests to future environmental conditions.

GRAPHICAL ABSTRACT

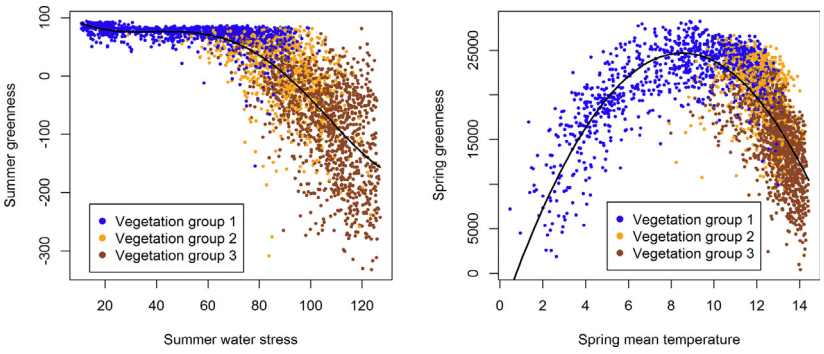

ARTICLE INFO

Article history:
Received 20 July 2018
Received in revised form 4 October 2018
Accepted 4 October 2018
Available online 11 October 2018

Editor: Frederic Coulon

Keywords:
Climate
Drought stress
Soil nutrition
NDVI
Vegetation
Stand types

ABSTRACT

Several studies use satellite-based normalized difference vegetation index (NDVI) to monitor the impact of climate change on vegetation covers. Good understanding of the drivers of NDVI patterns is hindered by the difficulties in disentangling the effects of environmental factors from anthropogenic changes, by the limited number of environmental predictors studied, and by the diversity of responses according to periods and land covers. This study aims to improve our understanding of the different environmental drivers of NDVI spatial variations for different stand type characteristics of mountain and Mediterranean biomes. Using NDVI values extracted from MODIS Terra time series, we calculated Spring Greenness (SG) and annual Relative Greenness (RGRE) to depict spring and summer vegetation activity, respectively, in a contrasted area of 10,255 km^2 located in the south of France. We modeled SG and RGRE at different scales, using 20 environmental predictors characterizing available energy, water supply, and nutrient supply calculated for different periods of the year. In spring, high minimum temperatures, good nitrogen availability, and acidic or neutral pH turned out to be determining for greenness, particularly for stand types located in altitude. In summer, an important soil water reserve and low temperatures promoted vegetation dynamics, particularly for stands located in areas with a Mediterranean climate. Our results show that NDVI dynamics was not only driven by climatic variability, and should not be studied using only mean temperature and rainfall. They highlight that different environmental factors act complementarily, and that soil parameters characterizing water stress and soil nutrition should be taken into account. While the factors limiting NDVI values varied according to the season and the position of the stands along the ecological gradients, we identified a global temperature and water-stress threshold when considering the whole vegetation.

© 2018 Elsevier B.V. All rights reserved.

* Corresponding author.
E-mail addresses: christian.piedallu@agroparistech.fr (C. Piedallu), veronique.cheret@purpan.fr (V. Chéret), jp.denux@purpan.fr (J.P. Denux), vincent.perez@agroparistech.fr (V. Perez), jaime4@ualberta.ca (J.S. Azcona), ingrid.seynave@inra.fr (I. Seynave), jean-claude.gegout@agroparistech.fr (J.C. Gégout).

https://doi.org/10.1016/j.scitotenv.2018.10.052
0048-9697/© 2018 Elsevier B.V. All rights reserved.

1. Introduction

More and more studies highlight the effects of the global climate change on vegetation (Boisvenue and Running, 2006; Lenoir et al., 2008; Vennetier and Ripert, 2009). They demonstrate important impacts on plant distribution, phenology, and productivity (Charru et al., 2014; Gordo and Sanz, 2010), with raising concerns about the vulnerability of natural ecosystems (Allen et al., 2010; Carnicer et al., 2011). In this context, identifying the different environmental factors that control vegetation dynamics and understanding their relative importance is a central issue. The Normalized Difference Vegetation Index (NDVI) is based on the differential absorption of red and near-infrared spectral bands (Rouse et al., 1973; Tucker et al., 1985), and quantifies vegetation greenness as related to vegetation vigor and extent (Luo et al., 2016; Rhee and Im, 2017). It is strongly correlated to the photosynthetically active radiation absorbed by vegetation, and it is recognized as an indicator of vegetation productivity. Since NDVI is linked to vegetation leaf area and chlorophyll content, it varies according to the vegetation type, the extent of the vegetation cover, the soil, geomorphology, CO_2 concentrations, nitrogen deposition, and climatic constraints (Kawabata et al., 2001; Wang et al., 2003).

NDVI is widely used in large-scale studies to determine vegetation dynamics and the responses of vegetation to climate. Time series of NDVI showed great interannual variability and contrasted evolutions according to the location, the scale, and the period, suggesting that multiple causes may interact (Fensholt et al., 2012). An increasing trend has been globally found worldwide over the last decades, e.g. in China (Meng et al., 2011), northern Europe (Julien et al., 2006), or Australia (Fensholt et al., 2012), with a succession of greening and browning periods (Liu et al., 2015). In other parts of the world like southern Europe (Julien et al., 2006), rainforests of South America and Africa (Liu et al., 2015), a decreasing trend has sometimes been observed.

The drivers of NDVI spatial patterns or trends have been intensively studied in the literature. Increasing trends in NDVI are most often attributed to the lengthening of the growing season due to warmer climate, which increases plant photosynthesis (Slayback et al., 2003). But increasing temperatures have also recently been found related to an NDVI decrease in humid temperate and dry areas (Liu et al., 2015). In boreal regions, the positive effect of increasing temperatures can be offset by the lack of light availability or by regional cooling (Forkel et al., 2015). Rainfall plays a minor role to explain NDVI in the literature. A positive link is generally observed, with a stronger relationship in arid areas than in colder and wetter areas (Peled et al., 2010; Vicente-Serrano et al., 2013). Some studies have also found no link or a negative relationship between NDVI and rainfall (Fensholt et al., 2012; Guo et al., 2014).

Our understanding of the causes of observed NDVI patterns and trends remains largely incomplete. Most studies have been hampered by the difficulties in disentangling the effects of environmental factors from the anthropogenic changes linked to land use changes or management practices like irrigation or fertilization (Zewdie et al., 2017), or the temporal variations in CO_2 fertilization (Fensholt et al., 2012). Although distinct NDVI responses were demonstrated according to vegetation nature and structure (Djebou et al., 2015), most of the studies were conducted at the biome or plant functional type scale, and made no distinction among the different land covers. The correlations between NDVI trends and mean temperature or rainfall are well documented (Luo et al., 2016), but the effects of other predictors have often been neglected. A wide range of climate and soil drivers playing a physiological role admittedly influence plant phenology or productivity (Seynave et al., 2005; Vallet and Perot, 2016), but their ability to explain greenness patterns is little known. Rainfall and temperature are often studied separately, although they both contribute to determine water availability for vegetation through the water balance, a key parameter to determine plant health and growth (Bigler et al., 2006; Breda et al., 2006). A few studies stressed the need to take into account both thermal and hydric constraints to understand NDVI variations owing to complex interactions between these factors (Piao et al., 2014), but they were rarely taken into account jointly. Finally, soil-related effects are often ignored in NDVI studies because it is difficult to obtain data, although the soil water regime and soil nutrition are probably key parameters to evaluate vegetation dynamics (Bergès and Balandier, 2010; Walker et al., 2003).

The aim of this article is to assess the environmental drivers of the vegetation dynamics at different scales and over different periods of the year, using a spatial approach. We studied the relationships between NDVI and environmental factors at the scale of the whole natural vegetation of the area, for 3 phenological groups, and across 15 stand types. These stand types were characteristic of mountain and Mediterranean biomes, and included coniferous as well as broadleaf and evergreen xerophilous tree species. We hypothesized that i) mean temperature and rainfall might not be the best predictors of NDVI patterns, ii) different factors could complement one another to explain NDVI variations, and iii) the relationships between NDVI and the ecological factors could vary according to the season, the scale, and the stand type. This study was carried out in the south of France along a climate gradient covering a wide range of altitudes (0 to 2800 m). We used two NDVI indices, i.e. Spring Greenness (SG) and Relative Greenness (RGRE), obtained from MODIS Terra time series and calculated yearly from 2000 to 2012, to investigate the effects of climate and soil conditions on spring and summer vegetation dynamics.

2. Materials and methods

2.1. Study site

The study area was located in the south of France, in the Aude and Pyrénées-Orientales districts (Occitanie region). It covered 10,255 km^2, with low anthropogenic pressure (garrigue or maquis, forests, Fig. 1). With altitudes ranging between 0 and 2800 m, the area was very heterogeneous, including Mediterranean climate near the sea with warm and dry summers, and mountainous areas with cold temperatures and heavy rainfalls. Over the 2000–2012 period, mean annual temperatures ranged from 3 to 15 °C, and the average sum of annual rainfall from 450 to 2000 mm (data from the meteorological weather stations, Météo France).

2.2. NDVI data

We used a series of MODIS Terra 16-day composite images (MOD13Q1 collection 5 product) at 250 × 250 m resolution, the highest provided by this satellite. The Constrained View angle - Maximum Value Composite (CV-MVC) technique is utilized by NASA to generate this MOD13Q1 product. It selects the observation with the highest NDVI and the smallest view angle to correct cloud contamination, directional reflectance, sun angle and shadow effects, and aerosol and water-vapor effects (Huete et al., 2002). We selected 296 NDVI syntheses acquired from February 2000 to December 2012. Dataset pre-processing included clipping the images to the study area, and re-projecting the images onto the French geodesic system. The remaining noise in the NDVI data series was corrected using the adaptive Savisky-Golay algorithm with TIMESAT Software (Jönsson and Eklundh, 2004).

We calculated two synthetic indices from the temporal variations of NDVI values to reflect seasonal vegetation activity (Chéret and Denux, 2011). Spring greenness (SG, Pettorelli et al., 2005, Reed et al., 1994) is the sum of NDVIs calculated for a fixed period of five NDVI syntheses from the onset of spring greenness (at the beginning of April) to the NDVI maximum (in June) before the dry season. (Appendix A). This represents vegetation activity during the period of maximum activity, with values ranging between 1.5 and 4.3, the higher values corresponding to more active vegetation:

$$SG = \sum \text{NDVI April to June} \quad (1)$$

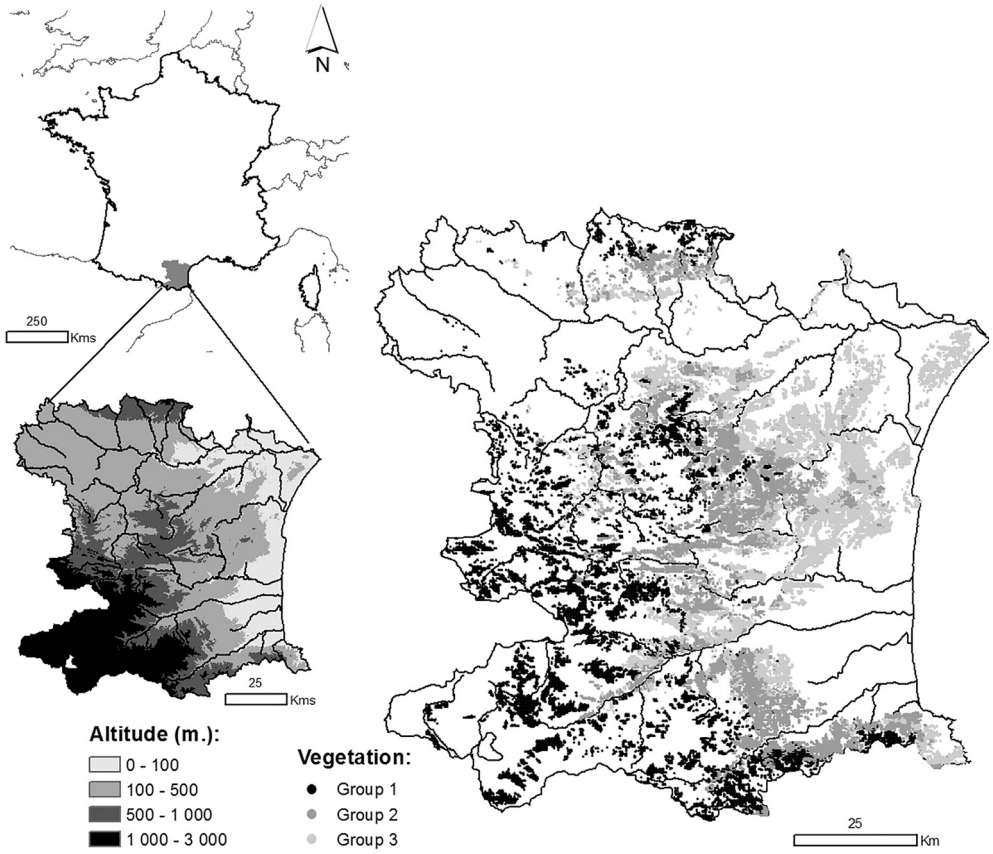

Fig. 1. Location of the study site, and distribution of altitudes and cells classified according to the 3 phenological vegetation groups (n = 2649).

Annual Relative Greenness (RGRE, Chéret and Denux, 2007, Kogan et al., 2003) is designed to represent the effects of summer constraints. It is obtained from the minimum NDVI measured before the onset of spring greenness (March–April) (Phase 1), the maximum NDVI observed at the end of spring (June), and the minimum NDVI reached during the driest period (August or September) (Phase 2) (Appendix A). It is calculated as follows:

$$\text{Annual RGRE} = (\text{NDVImin Phase 2} - \text{NDVImin Phase 1}) \div (\text{NDVImax} - \text{NDVImin Phase 1}) \quad (2)$$

with NDVImin Phase 1 = onset of spring greenness, NDVImax = end of spring greenness, NDVImin Phase 2 = end of summer decrease.

RGRE values range between −500 to 100. Positive values show a higher NDVI at the end of the summer decrease than at the onset of spring greenness, while negative values indicate that stress is so high in summer that vegetation decreases its activity to values lower than at the onset of spring greenness. RGRE and SG indices were resampled using a bilinear method at a cell size of 1 km for their resolution to match with GIS ecological indices.

2.3. GIS ecological indices

We calculated twenty ecological indices characterizing available energy, water availability, and soil nutrition, and mapped them at 1 km resolution (Table 1).

2.3.1. Climatic data

Mean, minimum, and maximum monthly temperatures (Tmean, Tmin, and Tmax), and the monthly sum of rainfalls (R) were gathered at the scale of France from 214, 225, 235, and 1119 weather stations, respectively, belonging to the Météo-France network. All the temperature records and 93% of rainfall records were subjected to statistical homogenization to remove non-climatic changes (Gibelin et al., 2014). These variables were modeled using geographically weighted regression (GWR, Fotheringham et al., 2002) for the whole of France at 1000 m resolution, using various covariates such as latitude, solar radiation, topographical position, wind exposure, or land use. We calculated monthly solar radiation (RAD) using the Helios model (Piedallu and Gégout, 2007) and combined it with temperatures using Turc's formula to obtain potential evapotranspiration (PET) (Turc, 1961). The difference between R and PET defined the climatic water balance (CWB).

2.3.2. Soil available water

To account for soil characteristics when estimating available water for plants, we calculated the soil water-holding capacity (SWHC). SWHC, which represents the maximum amount of water available for plants in the soil, was mapped from 100,307 plots all over France, collected by the French National Forest Inventory (NFI), and was implemented for France at 1 km resolution using pedotransfer functions (Piedallu et al., 2011). Then we calculated 6 soil water-balance indices among the most commonly used ones for each month (Dyer, 2009; Granier et al., 1999; Stephenson, 1998): Actual evapotranspiration (AET), available water (Soil Water Content, SWC, Relative Extractible Water, REW) or water stress (Evapotranspiration Deficit, ED, Soil Water Deficit, SWD, Aridity Index, AI) (Table 1).

2.3.3. Topography and bio-indicator indices

We added six complementary indices describing topography or soil properties. Cosine of aspect (Cosa) captures the difference between northern and southern slopes, and complemented the set of variables

Table 1
Indices and their ranges of values, defined by the first and ninth deciles (n = 2649).

	Index	Abb.	Definition	Frequency of calculation	Range	Reference
Energy	Mean temperature (°C)[a]	Tmean	Mean monthly temperatures	Monthly	[11; 18]	(Piedallu et al., 2016)
	Minimum temperature (°C)[a]	Tmin	Minimum monthly temperatures	Monthly	[6; 12]	
	Maximum temperature (°C)[a]	Tmax	Maximum monthly temperatures	Monthly	[16; 24]	
	Solar radiation (J/cm^2)[a]	RAD	Mean monthly solar radiation	Monthly	[53,100; 59,500]	
	Potential evapotranspiration (mm)[a]	PET	$PET_t = (\alpha * (RAD_t / D_t * 0.2388 + 50)) * (T_t / (T_t + 15))$ With $\alpha = 0.37$ for February, otherwise 0.4 D = number of days	Monthly	[54; 114]	(Turc, 1961)
	Actual evapotranspiration (mm)[a]	AET	If $P_t \geq PET_t$ then $AET_t = PET_t$ If $P_t \leq PET_t$ then $AET_t = SWC_{t-1} + P_t\text{-}SWC_t$	Monthly	[41; 65]	(Stephenson, 1998)
	Cosine of aspect	Cosa	Cosa = cos(aspect)	Constant over time	[−0.5; 0.5]	
Available water	Rainfall (mm)[a]	R	Sum of mean monthly rainfalls	Monthly	[38; 102]	(Piedallu et al., 2016)
	Climatic water balance (mm)[a]	CWB	$CWB_t = P_t - PET_t$	Monthly	[−69; 27]	(Stephenson, 1990)
	Soil water-holding capacity (mm)	SWHC	Amount of water that can be stored in the soil	Constant over time	[44; 71]	(Piedallu et al., 2011)
	Soil water content (mm)[a]	SWC	If $P_t \geq PET_t$ then $SWC_t = \min(SWC_{t-1} + CWB_t$ and SWHC) If $P_t \leq PET_t$ then $SWC_t = SWC_{t-1} * \exp((CWB_t) /$ SWHC)	Monthly	[2; 68]	(Thornthwaite and Mather, 1955) (Piedallu et al., 2013)
	Relative extractible water (mm)[a]	REW	$REW_t = SWC_t / SWHC$	Monthly	[0.18; 0.64]	(Granier et al., 1999)
	Aridity index (mm)[a]	AI	$AI_t = AET_t / PET_t$	Monthly	[0.45; 0.84]	(Thornthwaite and Mather, 1955)
	Evapotranspiration deficit (mm)[a]	ED	$ED_t = PET_t - AET_t$	Monthly	[15; 68]	(Dyer, 2009)
	Soil water deficit (mm)[a]	SWD	$SWD_t = 0.4 * SWHC\text{-}SWC_t$	Monthly	[−13; 11]	(Granier et al., 1999)
	Topographic wetness index	TWI	TWI = ln(a / Tan b) a = upslope area, b = slope in radians	Constant over time	[4.6; 6.5]	(Beven and Kirkby, 1979)
	Temporary waterlogging	TW	Bioindication with flora	Constant over time	[−0.032; −0.015]	(Piedallu et al., 2016)
	Permanent waterlogging	PW	Bioindication with flora	Constant over time	[−0.028; −0.018]	
Soil nutrition	Soil richness	pH	Bioindication with flora	Constant over time	[5.8; 7.9]	
	Nitrogen availability	C/N	Bioindication with flora	Constant over time	[13.7; 25.2]	

[a] For climatic data, the range column was calculated using mean monthly values from March to September, averaged over the 2000–2012 period. Abb. = abbreviation, t = month.

describing available energy for plants. The topographic control on hydrological processes was described by the Topographic Wetness Index-TWI (Beven and Kirkby, 1979). We also used four maps elaborated with bio-indicator indices: temporary and permanent waterlogging (respectively TW and PW), pH, and the C/N ratio (Gegout et al., 2003; Piedallu et al., 2016). These maps were calculated using >100,000 NFI plots with floristic inventories. TW and PW range from −1 to 1, with lower values when more drought-tolerant species are present. In the Mediterranean context of our site, they only presented negative values (Table 1), that we may interpret as drought indices. The pH and the C/N ratio respectively characterize soil acidity and nitrogen availability.

2.3.4. Calculating climatic data per period

For each year over the 2000–2012 period, the variables including climate data (Table1), which were calculated monthly, were averaged per period:

- for SG: spring (spr: March to May), the growing season (gs: March to June), the year (January–June),
- for RGRE: spring (spr: March to May), the growing season (gs: March to September), summer (su: June–August), and the year (year: January–September).

The combination of indices with periods led us to evaluate 46 and 59 candidate predictors to explain SG and RGRE, respectively, which were extracted for each plot from the GIS layers.

2.4. Dataset creation

For the 3146 initial 1-km^2 cells corresponding to forests, garrigue, or maquis according to the NFI map,[1] we extracted SG, RGRE, and the calculated ecological indices. Cells affected by land use changes or forest fires were removed by cumulating Corine Stand type changes recorded comparing 2000 to 2006 and then 2006 to 2012.[2] Each of the 2649 remaining cells were classified into three different vegetation groups according to yearly vegetation activity curves expressed by NDVI (Chéret and Denux, 2011), and to 15 stand types according to the NFI forest maps (Table 2, Fig. 1). Group 1 (n = 888) was composed of mountain coniferous and deciduous species, with mainly *Pinus uncinata*, *Abies alba*, *Fagus sylvatica*, or *Quercus* stands (Table 2). Group 2 (n = 814) corresponded a group of Mediterranean xerophilous species, the main species were *Quercus ilex* or *Q. suber*. Group 3 (n = 947) included non-wooded garrigue or maquis and a few Mediterranean coniferous stands with *Pinus halepensis* and *P. pinaster*.

2.5. Modeling design

We explored the links between SG, RGRE, and the selected ecological indices using a modeling approach based on linear regression. The analysis was carried out in two steeps: i) to determine the best predictors correlated to vegetation greenness in spring and summer, we evaluated

[1] http://inventaire-forestier.ign.fr/spip/spip.php?rubrique53.
[2] http://www.eea.europa.eu/data-and-maps/data#c17=&c11=&c5=all&c0=5&b_start=0.

Table 2
Means and standard deviations (std) for SG, RGRE, rainfall, and mean temperature. All the values were calculated using means over the 2000–2012 period (n = 2649). Rainfall and temperature values were mean monthly values between March and September. Stand types were sorted based on increasing temperatures.

Vegetation groups	Stand types	n	SG		RGRE		Precipitation		Temperature	
			Mean	Std	Mean	Std	Mean	Std	Mean	Std
Group 1	High forest of *Pinus uncinata*	172	3.03	0.43	82	8	212	59	6.2	1.1
n = (888)	High forest of *Abies alba*	126	3.96	0.29	74	8	104	49	9.4	1.8
	High forest of *Pinus sylvestris*	50	3.56	0.27	69	12	104	39	9.8	2.3
	High forest of *Fagus sylvatica*	93	3.84	0.22	78	7	85	35	10.7	1.7
	Fagus sylvatica coppice	84	3.85	0.23	74	6	82	27	11.1	1.5
	Castanea sativa coppice	77	3.83	0.13	80	7	68	10	12.8	1.0
	Quercus sp. Coppice	216	3.72	0.26	59	31	65	7	13.7	0.8
	Garrigue/maquis with Quercus *pubescens*	70	3.41	0.30	48	28	62	5	14.2	0.8
Group 2	High forest of *Pinus nigra*	23	3.76	0.25	48	26	61	5	14.0	0.7
n = (814)	*Quercus ilex* coppice	329	3.70	0.28	15	52	60	7	14.1	0.8
	Garrigue/maquis with Quercus *ilex/suber*	393	3.39	0.37	−26	67	58	9	14.5	0.9
	High forest of *Quercus suber*	69	3.51	0.29	6	45	50	3	15.5	0.9
Group 3	Garrigue/maquis non wooded	872	2.97	0.41	−83	89	51	9	15.1	0.9
n = (947)	High forest of *Pinus pinaster*	24	3.33	0.34	−49	56	48	7	15.4	0.4
	High forest of *Pinus halepensis*	51	2.79	0.32	−71	67	44	6	15.7	0.5

the links between SG and RGRE for each predictor separately, and ii) we determined if different predictors could complement one another using multivariate models. For these two approaches, models were built at three scales: i) the whole natural vegetation of the area, ii) the vegetation group, and iii) the stand type. For each model, we allowed the variables in linear and quadratic forms, corresponding to monotonic - increasing or decreasing - response curves, and bell-shaped response curves.

First, we evaluated the part of variance explained by each of the 46 and 59 indices for SG and RGRE, respectively. Each NDVI index was modeled for each year from the 2000–2012 period with the selected set of predictors, and the explained variance of the predictors was averaged over the 13 years. For each greenness index, the best-performing predictor was selected, and its relationships with SG and RGRE were described.

Secondly, we used multiple regressions to evaluate if different predictors could be complementary to explain NDVI spatial variations. Values from the 2000–2012 period were gathered in the same dataset for SG and for RGRE. For each model, we selected the best correlated ecological index step by step, until the newly added variable was not statistically significant ($P > 0.001$). To limit multicollinearity, a new variable was not selected if its correlation with the previously selected ones exceeded Pearson's $r = 0.7$, or if the shape of the response curve was inverted by the other variables and its ecological meaning became inconsistent with ecological knowledge (Rameau et al., 1989). For each model, the response curves were interpreted according to their ecological relevance (Appendix B). The relative importance of each regressor contribution was evaluated using the averaging over ordering method (lmg) (Lindeman et al., 1980), identified as one of the most relevant and available in the relaimpo package (Gromping, 2006). Database management and statistical analyses were performed using R 3.1.2 software.

3. Results

3.1. SG and RGRE variations

SG or RGRE values differed according to the vegetation, with globally decreasing values from group 1 to group 3, mainly for RGRE (Table 2). Vegetation responded to different patterns, with an important dynamic both in spring and summer for mountain coniferous and deciduous species, while Mediterranean xerophilous vegetation showed an SG increase in spring and various responses for RGRE in summer (Appendix C). In *Quercus ilex* and *Q. suber* stands, RGRE remained practically stable in summer, while it decreased in non-wooded garrigue or maquis and Mediterranean coniferous stands harboring *Pinus halepensis* and *P. pinaster*. Besides, the spring NDVI increase was lower for these stands than for the other stands. *Pinus uncinata* forests displayed a specific pattern, with lower activity in spring but high activity in summer.

For all stand types, SG variations among the different locations were relatively important (Table 2). For RGRE, stand types from group 1 were the most homogeneous, while stands from groups 2 or 3 showed the greatest standard deviation. This great variability mainly concerned the high forest of *Pinus halepensis*, *Pinus pinaster* or *Quercus suber*, *Quercus ilex* coppice, and non-wooded or *Q. suber* garrigue or maquis, suggesting various responses to environmental constraints.

3.2. Relationships between SG, RGRE, and each soil and climate predictor

Annual values of SG and RGRE were strongly linked to some of the selected environmental indices, with explained variance reaching 68% for SG and 45% for RGRE. Substantial differences were found according to predictors and vegetation (Table 3). The correlations with environmental variables were generally higher for SG than for RGRE, and were stronger for energy variables (mean or minimum temperatures, and PET). The predictors of the soil water balance were often the most correlated with RGRE, mainly for summer ED or AI, with increasing intensity from group 1 to group 3. Vegetation belonging to group 1 and located in the coldest areas showed different responses to climatic variables, with a better performance of climatic water indices (R or CWB) to explain SG, and energy variables (mainly temperatures or AET) to explain RGRE. These differentiated units were high forest of *Pinus uncinata*, *Abies alba*, *Pinus sylvestris*, and *Fagus sylvatica* on the one hand, and *Fagus sylvatica* or *Castanea sativa* coppice on the other hand. RAD, Cosa, and PW were never among the best correlated variables. On the contrary, TW and soil nutrition (pH and C/N) regularly showed good performances and were among the most efficient variables, mainly for group 1 stands.

Spring Tmean and summer ED are most often the best predictors, so we selected them to further describe the ecological constraints linked to SG (Fig. 2a) and RGRE (Fig. 2b), respectively. We observed a positive effect of spring Tmean on SG (mainly for the high forest of *Pinus uncinata*, Fig. 3a and Appendix Da) up to an optimum of 8 °C, but with a negative effect when spring Tmean increased beyond that point (mainly for vegetation groups 2 and 3). RGRE did not vary significantly when summer ED was lower than 70 mm (Fig. 3b), but decreased regularly where water stress grew more severe (stand types from groups 2 and 3 were mainly concerned; Figs. 2b and 3b, and Appendix Db).

Table 3
SG or RGRE variance explained by each of the 20 selected ecological indices (in %), for the whole site (All), the 3 vegetation groups, and the 15 stand types. The average value of explained variance calculated for each year of the 2000–2012 period is given for each index. Climatic data were calculated for different periods of the year, so only the best performance was reported, and the period was identified in brackets: Sp = spring, Su = summer, Gs = growing season, Yr = year. The highest 3 performances are highlighted in grey for each vegetation type, with the best performance in dark grey.

			Energy							Available water											Soil nutrition	
	SG	n	Tmean	Tmin	Tmax	RAD	PET	AET	Cosa	R	CWB	SWC	AI	ED	REW	SWD	SWHC	TWI	TW	PW	pH	C/N
	All	34168	53(Sp)	51(Sp)	35(Yr)	06(Gs)	48(Gs)	25(Gs)	1	29(Gs)	39(Gs)	20(Sp)	37(Yr)	35(Yr)	32(Yr)	28(Gs)	1	19	26	14	36	4
	Group 1	11544	61(Sp)	60(Sp)	55(Gs)	10(Gs)	61(Sp)	57(Sp)	1	54(Yr)	60(Yr)	04(Gs)	44(Yr)	23(Yr)	28(Yr)	10 (Gs)	4	0	10	6	5	48
	Group 2	10313	25(Sp)	20(Sp)	17(Yr)	02(Yr)	19(Gs)	07 (Sp)	1	09 (Sp)	12 (Sp)	04 (Sp)	10(Gs)	12 (Yr)	08 (Yr)	07(Gs)	1	17	28	16	33	5
	Group 3	12311	39(Yr)	36(Yr)	21(Yr)	03(Gs)	31(Yr)	21(Gs)	0	26(Gs)	30(Gs)	15(Gs)	28(Yr)	30 (Yr)	25 (Yr)	23(Yr)	1	9	14	13	16	3
Group 1	High forest of Pinus uncinata	2236	42(Gs)	41 (Gs)	36 (Yr)	02 (Gs)	54 (Sp)	55 (Sp)	0	49 (Yr)	65 (Yr)	15 (Sp)	39 (Yr)	11 (Yr)	16 (Gs)	15 (Sp)	18	6	1	1	1	11
Group 1	High forest of Abies alba	1638	58 (Sp)	58 (Sp)	63 (Sp)	07 (Sp)	60 (Sp)	61 (Sp)	0	64 (Yr)	66 (Yr)	04 (Sg)	39 (Yr)	32 (Gs)	33 (Gs)	09 (Gs)	2	14	2	2	18	57
Group 1	High forest of Pinus sylvestris	650	42 (Gs)	42 (Sp)	52 (Gs)	22 (Gs)	58 (Sp)	54 (Sp)	6	47 (Yr)	52 (Gs)	11 (Gs)	36 (Gs)	35 (Gs)	36 (Yr)	18 (Gs)	4	2	12	3	25	57
Group 1	High forest of Fagus sylvatica	1209	42 (Sp)	39 (Sp)	48 (Gs)	17 (Sp)	33 (Sp)	30 (Sp)	4	46 (Yr)	53 (Yr)	14 (Sp)	26 (Yr)	23 (Gs)	25 (Yr)	12 (Sp)	26	8	2	12	13	29
Group 1	Fagus sylvatica coppice	1092	35 (Sp)	32 (Sp)	40 (Gs)	06 (Sp)	47 (Gs)	44 (Sp)	5	50 (Yr)	58 (Sp)	26 (Sp)	27 (Yr)	20 (Gs)	22 (Gs)	17 (Sp)	36	19	2	1	4	33
Group 1	Castanea sativa coppice	1001	25 (Gs)	25 (Gs)	09 (Gs)	19 (Gs)	04 (Gs)	22 (Gs)	2	25 (Sp)	17 (Sp)	12 (Sp)	24 (Gs)	22 (Gs)	19 (Gs)	15 (Gs)	9	1	12	5	4	6
Group 1	Quercus sp. Coppice	2808	28 (Gs)	29 (Yr)	26 (Yr)	02 (Sp)	18 (Yr)	09 (Sp)	0	06 (Sp)	10 (Yr)	04 (Sp)	07 (Sp)	08 (Sp)	07 (Yr)	05 (Gs)	2	4	6	2	7	6
Group 1	Garrigue/maquis Quercus pubescens	910	26 (yr)	25 (Sp)	23 (Yr)	01 (Gs)	13 (Yr)	09 (Yr)	2	12 (gs)	11 (Yr)	03 (Gs)	09 (Yr)	08 (Yr)	08 (Yr)	05(Sp)	8	4	1	1	1	13
Group 2	High forest of Pinus nigra	299	67 (Sp)	68 (Sp)	25 (Yr)	23 (Sp)	12 (Gs)	31 (Yr)	6	17 (Yr)	18 (Yr)	21 (Gs)	16 (Sp)	17 (Sp)	14 (Sg)	19 (Sp)	9	19	34	13	12	1
Group 2	Quercus ilex coppice	4277	21 (Sp)	17 (Sp)	19 (Gs)	04 (Gs)	14 (Gs)	07 (Sp)	0	06 (Sp)	07 (Yr)	03 (Sp)	04 (Sp)	05 (Sp)	04 (Sp)	04 (Yr)	2	11	11	1	18	2
Group 2	Garrigue/maquis Quercus ilex/suber	4840	34 (Yr)	34 (Sp)	22 (Yr)	03 (Gs)	18 (Sp)	14 (Gs)	1	18 (Yr)	21 (Yr)	12 (Gs)	19 (Yr)	20 (Sg)	17 (Yr)	15 (Yr)	2	11	12	14	16	2
Group 2	High forest of Quercus suber	897	26 (Gs)	17 (Sp)	33 (Yr)	14 (Sp)	32 (Gs)	15 (Sp)	6	16 (Yr)	23 (Yr)	11 (Sp)	20 (Yr)	24 (yr)	17 (Sp)	18 (Gs)	36	32	2	6	12	21
Group 3	Garrigue/maquis non wooded	11336	35 (Yr)	33 (Sp)	16 (Yr)	02 (Gs)	28 (Gs)	22 (Gs)	1	25 (Gs)	29 (Gs)	17 (Gs)	28 (Yr)	29 (Gs)	25 (Yr)	22 (Sp)	3	15	31	15	33	5
Group 3	High forest of Pinus pinaster	312	56 (Yr)	54 (Yr)	48 (Yr)	08 (Sp)	19 (Yr)	33 (Sp)	41	36 (Yr)	40 (Yr)	27 (Sp)	35 (Sp)	34 (Sp)	33 (Sp)	32 (Gs)	24	3	23	12	4	3
Group 3	High forest of Pinus halepensis	663	31 (Sp)	25 (Gs)	15 (Gs)	05 (Gs)	20 (Gs)	12 (Gs)	1	18 (Gs)	24 (Yr)	06 (Sp)	16 (Yr)	17 (Yr)	13 (Yr)	15 (Gs)	4	1	8	6	4	3

			Energy							Available water											Soil nutrition	
	RGRE	n	Tmean	Tmin	Tmax	SR	PET	AET	Cosa	R	CWB	SWC	AI	ED	REW	SWD	SWHC	TWI	TW	PW	pH	C/N
	All	34168	34 (Sp)	34 (Yr)	23 (Yr)	05 (Yr)	34(Su)	42(Su)	2	32(Su)	36(Su)	33(Sp)	42(Su)	45(Su)	36(Sp)	36(Sp)	1	18	16	7	38	4
	Group 1	11544	19(Sp)	18 (Yr)	18(Yr)	02 (Yr)	17 (Gs)	15 (Yr)	1	14 (Su)	17(Su)	08(Su)	15(Su)	17 (Yr)	14 (Gs)	13(Su)	3	4	1	1	13	11
	Group 2	10313	10 (Gs)	09 (Yr)	05 (Yr)	02 (Yr)	08 (Yr)	16 (Su)	1	14(Su)	17 (Su)	09 (Gs)	17 (Su)	18 (Su)	13 (Gs)	13 (Sp)	3	6	19	8	19	3
	Group 3	12311	15 (Gs)	16 (Gs)	05 (Yr)	05 (Su)	16 (Su)	26 (Su)	1	21 (Su)	24 (Su)	23 (Sp)	27 (Su)	27 (Su)	25 (Sp)	22 (Sp)	2	10	10	7	16	4
Group 1	High forest of Pinus uncinata	2236	12 (Gs)	12 (Gs)	10 (Gs)	03 (Yr)	15 (Gs)	17 (Gs)	3	15 (Yr)	08 (Yr)	08 (Gs)	13 (Yr)	09 (Su)	08 (Su)	08 (Sp)	9	2	5	2	8	6
Group 1	High forest of Abies alba	1638	14 (Su)	14 (Gs)	13 (Gs)	04 (Su)	12 (Sp)	11 (Yr)	0	14 (Yr)	14 (Yr)	08 (Su)	11 (Su)	11 (Su)	12 (Yr)	12 (Gs)	6	8	5	6	9	9
Group 1	High forest of Pinus sylvestris	650	27 (Su)	27 (Su)	26 (Su)	17 (Yr)	20 (Yr)	21 (Sp)	4	22 (Gs)	22 (Gs)	13 (Su)	22 (Yr)	19 (Gs)	22 (Yr)	15 (Gs)	3	5	4	5	11	24
Group 1	High forest of Fagus sylvatica	1209	05 (Gs)	06 (Gs)	06 (Gs)	06 (Su)	04 (Gs)	09 (Gs)	4	08 (Sp)	07 (Sp)	07 (Sp)	08 (Sp)	08 (Sp)	07 (Sp)	05 (Gs)	6	6	4	3	6	5
Group 1	Fagus sylvatica coppice	1092	19 (Gs)	18 (Gs)	21 (Gs)	05 (Yr)	15 (Gs)	16 (Su)	3	17 (Su)	18 (Su)	07 (Su)	18 (Su)	20 (Yr)	14 (yr)	13 (Gs)	6	9	6	5	19	18
Group 1	Castanea sativa coppice	1001	15 (Sp)	13 (Gs)	13 (Gs)	05 (Gs)	07 (Yr)	13 (Gs)	5	14 (Gs)	15 (Gs)	11 (Yr)	11 (Sp)	12 (Su)	11 (Yr)	11 (Yr)	1	11	27	3	27	13
Group 1	Quercus sp. Coppice	2808	08 (Gs)	08 (Sp)	08 (Su)	02 (Su)	08 (Su)	08 (Su)	1	08 (Su)	08 (Su)	05 (Su)	11 (Gs)	11 (Gs)	10 (Gs)	08 (Gs)	1	9	3	2	1	2
Group 1	Garrigue/maquis Quercus pubescens	910	06 (Gs)	06 (Gs)	06 (Gs)	02 (Gs)	07 (Su)	12 (Su)	7	16 (Su)	15 (Su)	04 (Gs)	11 (Su)	11 (Su)	06 (Sp)	13 (Su)	16	4	3	3	5	15
Group 2	High forest of Pinus nigra	299	30 (Gs)	29 (Gs)	20 (Su)	26 (Gs)	12 (Yr)	22 (Gs)	23	24 (Su)	19 (Su)	19 (Yr)	21 (Su)	19 (Su)	15 (Su)	21 (Su)	15	1	29	12	17	17
Group 2	Quercus ilex coppice	4277	07 (Gs)	05 (Gs)	07 (Gs)	03 (Gs)	08 (Gs)	07 (Gs)	1	10 (Su)	12 (Su)	04 (Gs)	11 (Su)	12 (Su)	10 (Gs)	10 (Gs)	3	14	5	8	1	6
Group 2	Garrigue/maquis Quercus ilex/suber	4840	16 (Gs)	18 (Gs)	09 (Yr)	04 (Gs)	15 (Gs)	24 (su)	1	19 (Gs)	22 (Su)	18 (Gs)	25 (Gs)	26 (Su)	23 (Gs)	21 (Gs)	3	14	15	4	18	4
Group 2	High forest of Quercus suber	897	09 (Su)	14 (Su)	10 (Su)	06 (Gs)	05 (Su)	20 (su)	3	19 (Su)	15 (Gs)	04 (Yr)	18 (Su)	14 (Su)	09 (Sp)	13 (Gs)	4	1	1	1	1	16
Group 3	Garrigue/maquis non wooded	11336	17 (Yr)	18 (Su)	06 (Yr)	04 (Su)	17 (Su)	29 (Su)	1	23 (Su)	26 (Su)	27 (Gs)	30 (Su)	31 (Su)	28 (Gs)	25 (Yr)	5	7	21	8	22	4
Group 3	High forest of Pinus pinaster	312	20 (Su)	21 (Sp)	25 (Su)	18 (Yr)	15 (Yr)	15 (Yr)	13	15 (Su)	15 (Su)	12 (Gs)	17 (Sp)	15 (Su)	17 (Yr)	17 (Yr)	12	16	18	7	14	13
Group 3	High forest of Pinus halepensis	663	10 (Gs)	15 (Gs)	18 (Su)	10 (Gs)	12 (Yr)	19 (Su)	2	15 (Su)	16 (Su)	19 (Yr)	19 (Su)	20 (Su)	19 (Gs)	17 (Yr)	5	9	16	9	11	2

3.3. Explaining SG and RGRE spatial variations using multivariate models

Our models performed better for SG (with an explained variance ranging from 18 to 70% for the different stand types) than for RGRE (8 to 42%). For SG, performance tended to decrease from group 1 to 3, while it tended to increase for RGRE, for which group 3 had the best performing models (Fig. 4a and b). With between 2 and 6 predictors per model, we showed that different variables were always complementary to explain greenness indices, but with substantial differences between SG and RGRE (Appendices E and F). Mild climates promoted spring greenness, particularly for the stand types belonging to group 1 (Fig. 4a). The need for heat in spring is most often identified by an increasing response curve to Tmin or PET (Fig. 5a). It is complemented in a lower proportion by the need for moisture and cool temperatures, represented in models by annual solar radiation or mean annual temperatures; their increase causes SG to decrease.

High moisture availability was the most determining variable to explain high RGRE values, with growing intensity from group 1 to group 3 (Fig. 4b). It was complemented by coolness, as RGRE decreased when temperatures were hot. Soil water balance predictors (mainly AI or ED) were the most efficient variables to characterize moisture availability for RGRE, but climatic variables (CWB or P), site characteristics (SWHC, TWI), and TW were also selected to model both SG and RGRE (Fig. 5b). Moisture variables using climate information were often complemented by variables describing the local soil water reserve or lateral fluxes (SWHC, TWI). Soil nutrition also had a substantial effect, mainly on SG, with a positive effect on greenness when nitrogen availability was good and when the pH was acidic for the vegetation of group 1, and neutral for the vegetation of groups 2 and 3 (Fig. 4a).

4. Discussion

By using a spatial approach, selecting stand types with reduced human activities, and removing areas submitted to land use changes, we avoided the influence of CO_2 variations and limited the influence of anthropogenic factors, and were able to focus on abiotic stresses that limit vegetation dynamics. We identified the most influential ecological factors that limit spring and summer NDVI variations of the vegetation characteristics of mountain and Mediterranean biomes, with relevant differences between periods and stand types. We highlighted that different environmental factors should be taken into account to properly describe NDVI variations, including temperature, soil water availability, and soil nutrition.

Temperature was one of the most explanatory factors, but it acted in different ways according to the season, the scale, and the stand type. Greenness was positively correlated with temperature in spring for mountain coniferous and deciduous species, but negatively correlated when temperatures rose, mainly for Mediterranean garrigue or maquis and coniferous stands. The effect of winter frosts on vegetation activity is well known (Forkel et al., 2015), with a negative influence that reduces the length of the growing season (Jin et al., 2014), while hot temperatures are known to decrease photosynthetic activity (Hew et al., 1969). During hot periods, high temperatures complemented low water availability to limit greenness. This can appear as contradictory with studies stating that water stress – as opposed to heat stress – is primarily implied in the decline of primary productivity (Reichstein et al., 2007). Nevertheless, the negative effects of high temperatures on NDVI were already documented (Yao et al., 2018), and similar results have been found to explain NDVI changes (Buermann et al., 2014), tree productivity (Stangler et al., 2017), or plant distribution (Piedallu et al., 2016). In addition to the physiological effect of hot temperatures on plants, we probably selected temperature as a proxy of water stress because it is an important determinant of evapotranspiration, and evapotranspiration is an important component of the water balance easier to estimate than the soil water reserve.

We observed these opposite effects of temperatures between different periods or stand types along an altitude gradient, but also within a given stand type. For example, high *Pinus pinaster* forest exhibited a positive response of RGRE to Tmin and a negative one to Tmean (Appendix F). These results can be related to studies about plant phenology or growth (Zhou et al., 2016). For example, Seynave et al. (2008) modeled the *Fagus sylvatica* site index and found a positive link with May temperatures and a negative one with July temperatures. When using mean temperatures, only the combination of these opposite effects is observed, and this can hide the smaller effects or weaken the link with temperature, as recently observed in different studies (Liu et al., 2015; Piao et al., 2014). We therefore recommend to include indices characterizing both frost and warm conditions to properly study NDVI patterns and trends.

Water availability was also one of the main drivers of vegetation greenness in our models for the spring period as well as for the summer period, but even more so for the stands and seasons for which moisture was a limiting factor. This result is consistent with the decline of the vitality of certain tree species already observed in areas where rainfalls decrease (Scharnweber et al., 2011), with a higher sensitivity to moisture in dry regions (Chen et al., 2014). We showed important differences in performances between the different variables describing the

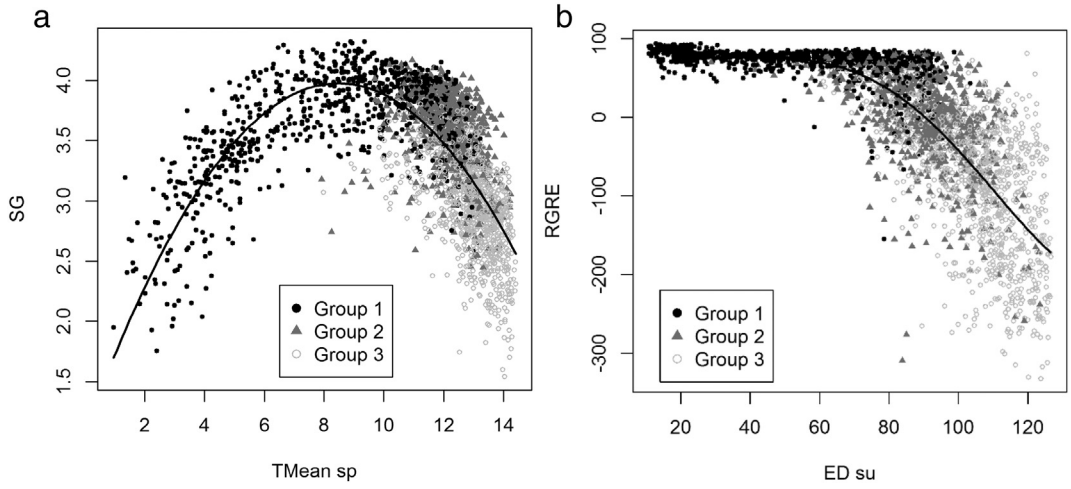

Fig. 2. Relationships between SG and spring Tmean (Tmean sp, a), RGRE and summer evaporation deficit (ED su, b) for the three vegetation groups. Each dot represents the average values over the 2000–2012 period (n = 2649).

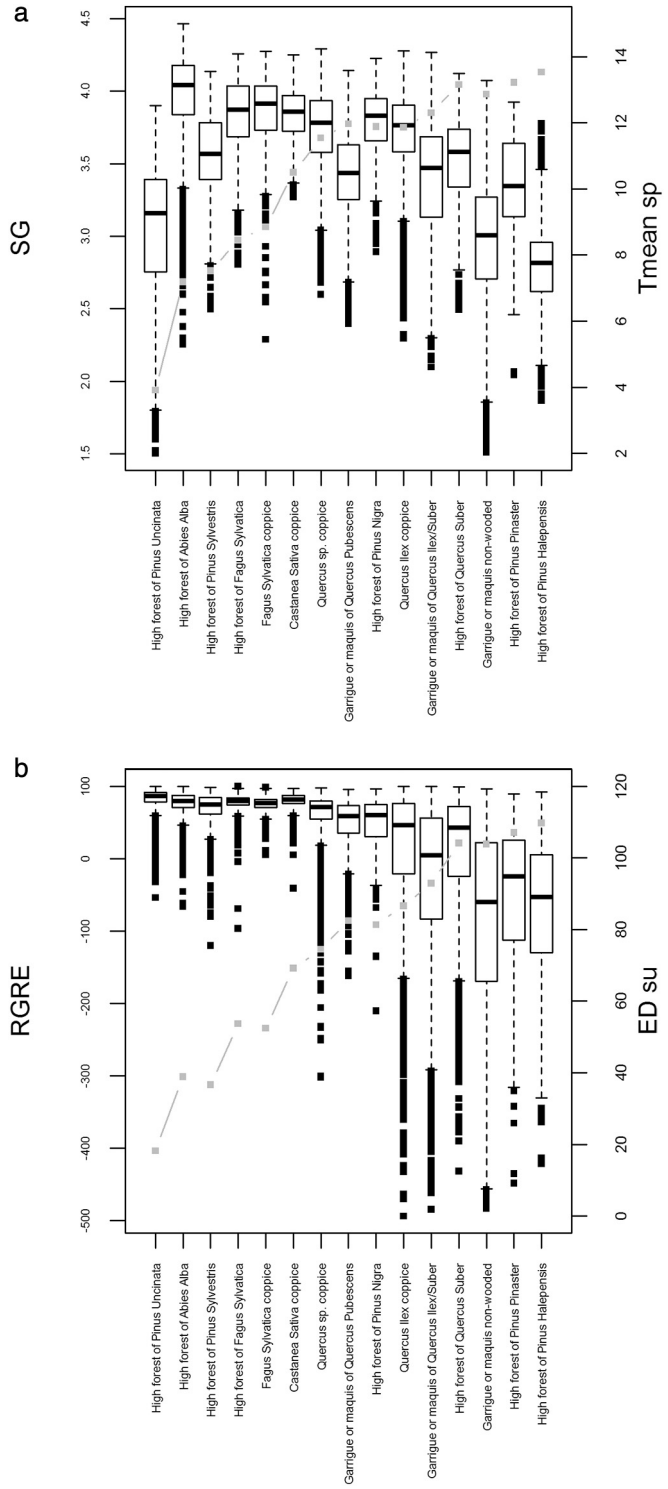

Fig. 3. Distribution of SG (a) and RGRE values (b) across the 15 stand types. Each boxplot represents data from the 13 years over the 2000–2012 period (n = 34,168). The grey line represents the average spring Tmean and summer ED for each stand type.

water constraint for plants. We found that rainfall, which is the most commonly used water variable, globally showed poor performances as compared to water balance indices, which were particularly efficient to explain NDVI variations when they took the soil water reserve into account. The lower performance of rainfall could agree with the absence of a link or a negative relationship with NDVI found in many studies (Fensholt et al., 2012; Guo et al., 2014). This result supports those of Peled et al. (2010), who showed a good correlation of soil drought indices with NDVI at the European scale. These variables were also often complemented by data describing site characteristics (SWHC, TWI), in agreement with Dorman et al. (2013), who demonstrated an effect of local conditions in addition to regional environmental factors during wet periods. Using an index that integrates temperature and water is particularly important in the current climate change context, which is characterized by a global increase of temperatures, but with a more heterogeneous trend as regards rainfall (IPCC et al., 2013). The better performance of the soil water indices and the differential trends in temperature and rainfall in a climate change context lead us to warmly recommend evaluating soil water balance variables in NDVI studies.

Vegetation greenness was higher when nitrogen availability was good, and when the pH was acidic or neutral. A positive effect of nitrogen nutrition on plant growth had already been observed in agronomy and forestry (Bontemps et al., 2011), and experiments carried out on crops showed an influence on NDVI values (Zubillaga and Urricariet, 2005). In forests, a correlation between the leaf nitrogen content and NDVI has been established (Nestola et al., 2018), and recent studies showed that NDVI could be a predictor of soil nitrogen in a small watershed (Jeong et al., 2017). We showed that nitrogen availability also influenced NDVI patterns when studying large forested areas, and for different stand types. We quantified its effect, which was important in spring for stands belonging to vegetation groups 1 and 2, suggesting an increase in vegetation growth when climatic conditions are favorable (mean temperatures around 8 °C and limited water stress in spring). As for the pH, the bell-shaped response curve to SG for the stands harboring *Quercus ilex* or *Q. suber* or *Pinus pinaster* seemed relevant according to current knowledge about these species (Rameau et al., 2008). The higher greenness values related to low pH values, mainly found in the models for the whole vegetation or the 3 studied groups, was more surprising. However, it is consistent with the results of Walker et al. (2003), who found lower NDVI values in northern Alaska on non-acidic parent material comparatively to acidic soils. The authors attributed this shift to differences in species composition and mainly shrub phytomass. Since we conducted our research at the vegetation unit scale, differences in vegetation dynamics are a more likely explanation for our results. Different studies performed in a similar geographical context already evidenced a negative relationship between tree growth and pH values for different species (Charru et al., 2017; Seynave et al., 2008). The role played by soil acidity and nitrogen nutrition in our models demonstrates that it is important to include soil nutritional properties in research aiming to understand NDVI variations. If such variables are missing, long-term NDVI trends may be misinterpreted, and it may be impossible to disentangle the effects of climatic changes from those of nitrogen deposition or soil acidification.

Taking all the stands together, we found a global threshold of mean temperature and soil water availability beyond which greenness activity decreased for SG and RGRE, respectively. This can appear as contradictory with the fact that the different stand types did not exhibit the same dynamic or the same response to environmental factors. The position of each stand type along the large ecological gradient in our study probably determined the nature and the range of the ecological constraints. NDVI increased for high-altitude vegetation (mainly *Pinus uncinata*) mainly in summer, since spring frosts drastically reduced values. For vegetation from the montane belt (*Abies alba*, *Fagus sylvatica*, *Pinus sylvestris*, …), the ecological conditions of the site seemed optimal: heat, water stress, and frost constraints were low. The highest SG and RGRE values were found in this area, corresponding to regional optimal growth conditions, modulated according to nitrogen availability. For the vegetation mainly located at low altitudes and based on garrigue, maquis, and forests harboring *Quercus ilex*, *Q. suber*, *Pinus pinaster*, or *P. halepensis*, vegetation activity mainly occurred in spring, and then the summer heat and drought significantly decreased NDVI values. All these differences among stand types were not visible when studying

a

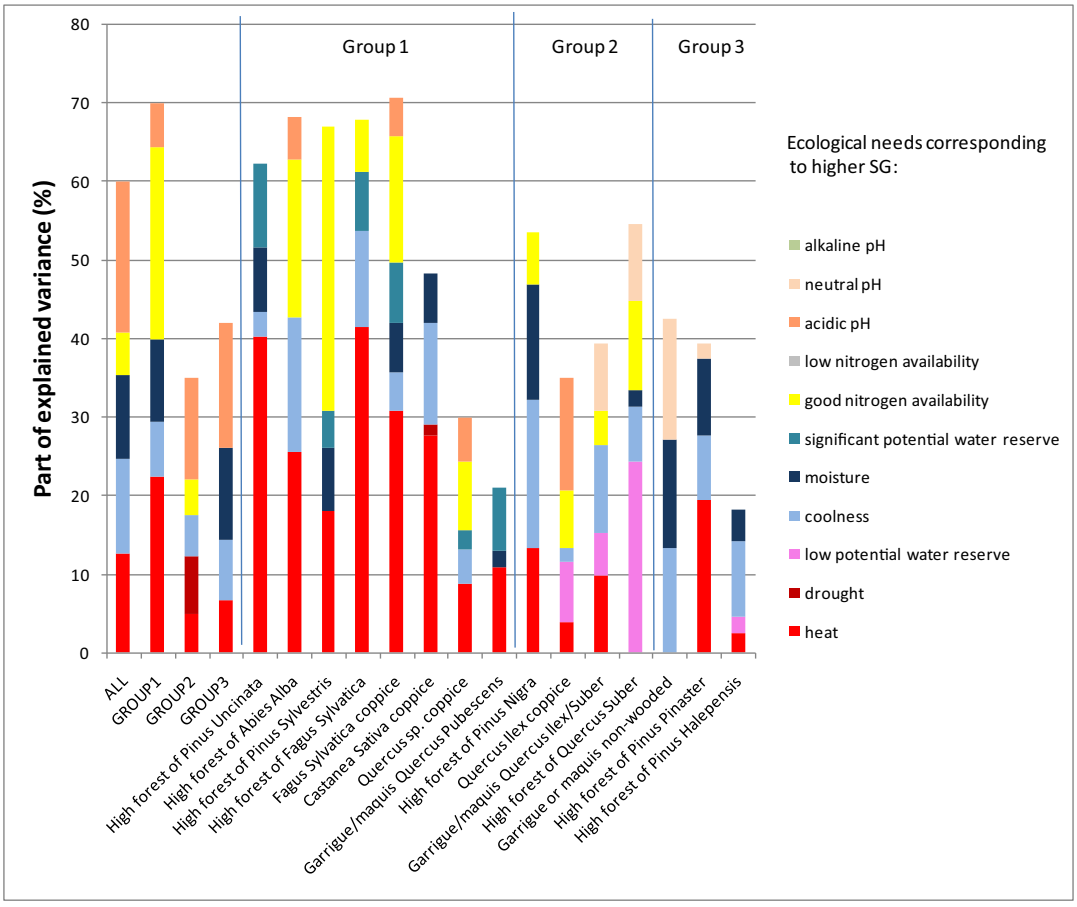
Group 1
Group 2
Group 3
Part of explained variance (%)
0
10
20
30
40
50
60
70
80
ALL
GROUP1
GROUP2
GROUP3
High forest of Pinus Uncinata
High forest of Abies Alba
High forest of Pinus Sylvestris
High forest of Fagus Sylvatica
Fagus Sylvatica coppice
Castanea Sativa coppice
Quercus sp. coppice
Quercus Pubescens
Garrigue/maquis Quercus Pubescens
High forest of Pinus Nigra
Quercus Ilex coppice
Garrigue/maquis Quercus Ilex/Suber
High forest of Quercus Suber
Garrigue or maquis non-wooded
High forest of Pinus Pinaster
High forest of Pinus Halepensis
Ecological needs corresponding to higher SG:
alkaline pH
neutral pH
acidic pH
low nitrogen availability
good nitrogen availability
significant potential water reserve
moisture
coolness
low potential water reserve
drought
heat

b

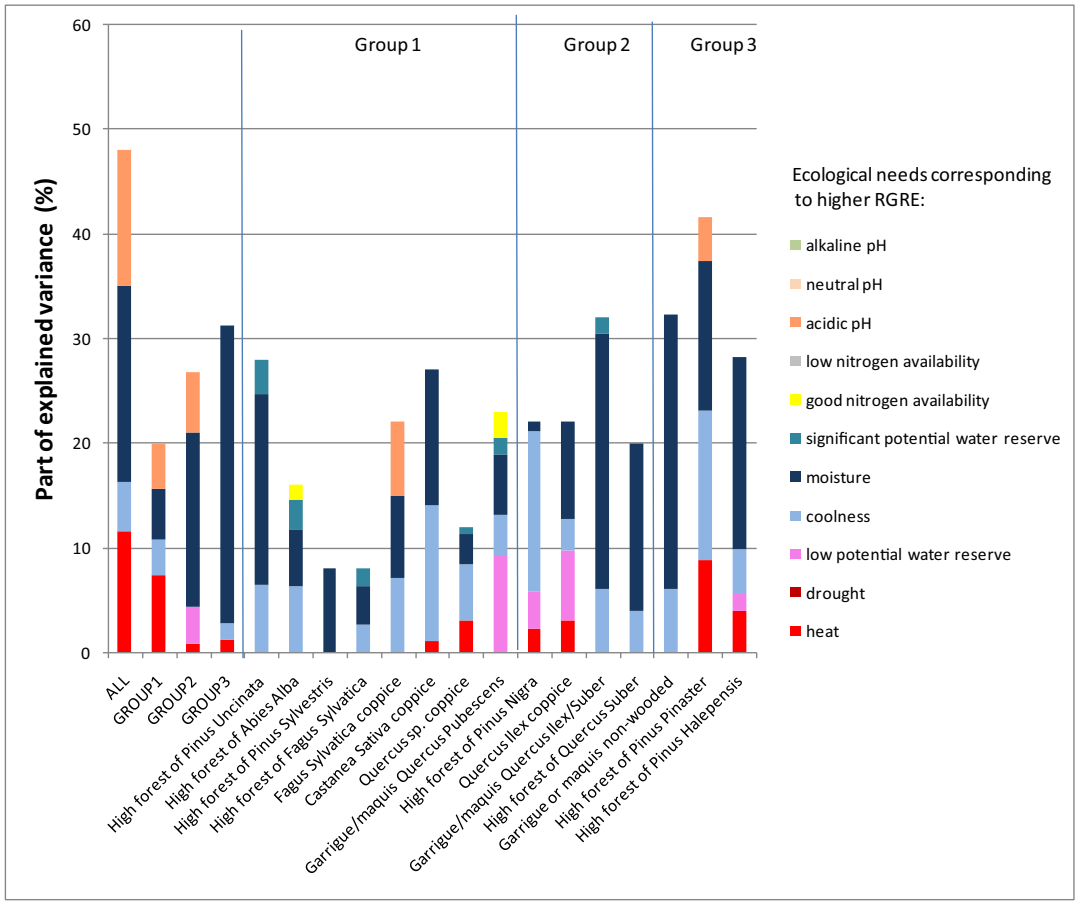
Group 1
Group 2
Group 3
Part of explained variance (%)
0
10
20
30
40
50
60
ALL
GROUP1
GROUP2
GROUP3
High forest of Pinus Uncinata
High forest of Abies Alba
High forest of Pinus Sylvestris
High forest of Fagus Sylvatica
Fagus Sylvatica coppice
Castanea Sativa coppice
Quercus sp. coppice
Quercus Pubescens
Garrigue/maquis Quercus Pubescens
High forest of Pinus Nigra
Quercus Ilex coppice
Garrigue/maquis Quercus Ilex/Suber
High forest of Quercus Suber
Garrigue or maquis non-wooded
High forest of Pinus Pinaster
High forest of Pinus Halepensis
Ecological needs corresponding to higher RGRE:
alkaline pH
neutral pH
acidic pH
low nitrogen availability
good nitrogen availability
significant potential water reserve
moisture
coolness
low potential water reserve
drought
heat

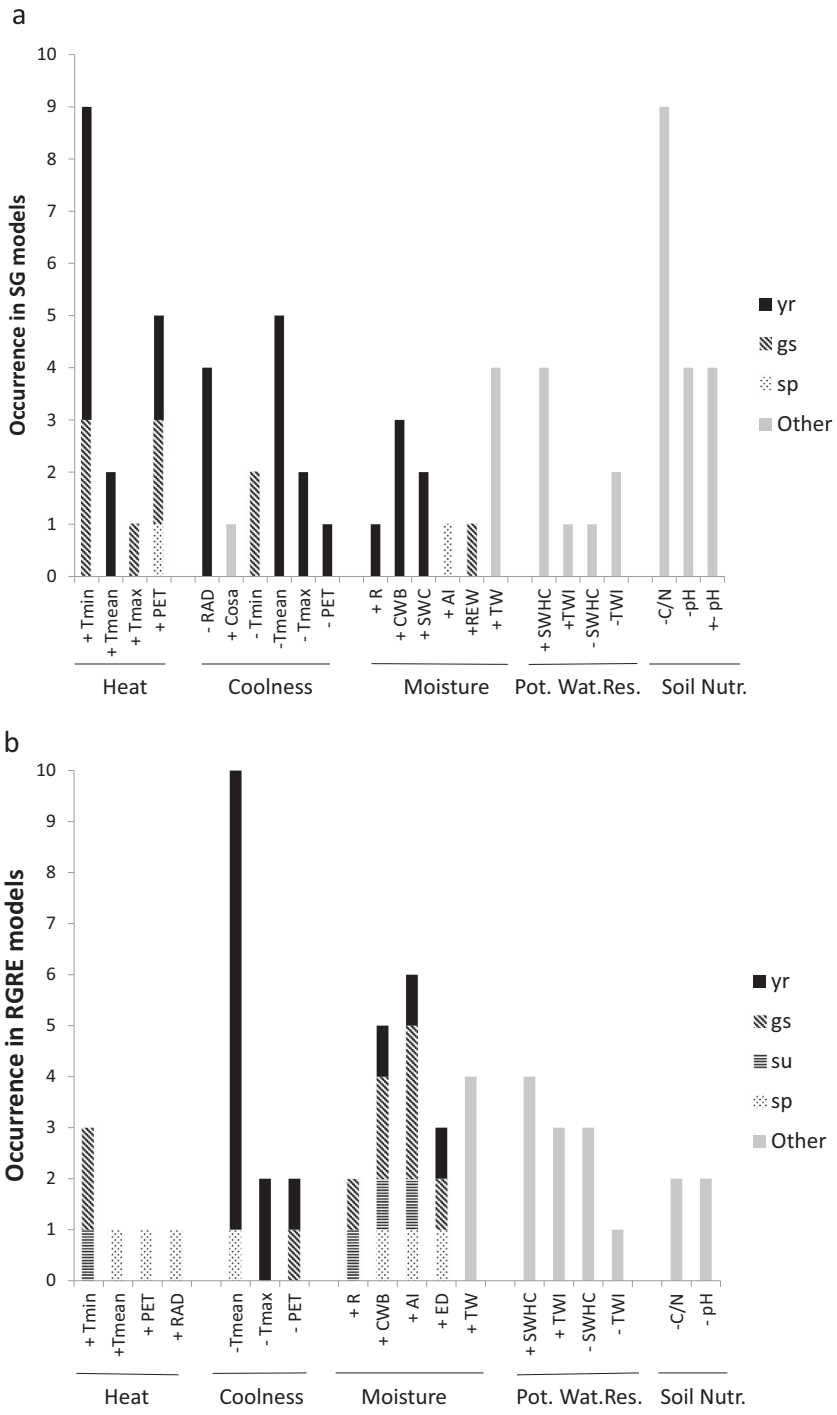

Fig. 5. Occurrence of the predictors selected to model SG (a) and RGRE (b), for the 15 stand types. Sp = spring, su = summer, gs = growing season, yr = year, other = predictors not linked to a specific period of the year, Pot.wat.res. = Potential water reserve, Soil nutr. = soil nutrition. The sign indicates the slope of the response curve.

the full vegetation cover or the vegetation groups. These findings complement at the regional scale the results of large-scale studies showing that the sensitivity of vegetation to temperatures and rainfall varies along these environmental gradients (Quetin and Swann, 2017). Our results strengthen previous studies identifying heterogeneous NDVI responses to the environment between land cover (Djebou et al., 2015) or forest productivity responses between tree species (Charru et al., 2017). They also highlight how important it is to study vegetation dynamics at a finer scale than the biome or plant functional type scales to properly identify NDVI drivers.

5. Conclusion

The responses according to stand types demonstrate that different factors can contribute to the vegetation dynamics in a complex way, suggesting that prediction of NDVI patterns or changes should include

Fig. 4. Assessment of the SG (a) and RGRE (b) responses to climate and soil factors for the whole vegetation of the site, the 3 vegetation groups, and the 15 stand types. The percentage of explained variance is expressed in terms of ecological needs for the vegetation: for example a red bar shows that heat promoted greenness activity. Data from the 13 years of the 2000–2012 period were used to calibrate the models (n = 34,168).

a combination of these different, possibly interacting drivers. The models elaborated in this study can be used to simulate potential consequences of future environmental changes for the different stand types, or can help to improve process-based models (Hui et al., 2014). They can also be used as decision-support tools for foresters and land managers to understand and monitor the consequences of climate or soil changes. Our findings suggest that a warmer climate can benefit to vegetation greenness up to a threshold temperature and when summer temperatures and water deficit remain low. These conditions correspond to vegetation currently located in the montane belt under Mediterranean climates. For vegetation located in warmer areas, a temperature increase, a decrease in soil water availability, or a combination of both, is expected to reduce vegetation dynamics both in spring and summer. These results are in agreement with studies showing a decrease of forest productivity in the Mediterranean context over the last decades (Charru et al., 2017). They also suggest that the greening observed under northern latitudes (Piao et al., 2011; Verbyla, 2008) could reverse if temperatures increase or water availability decreases, as already observed is some parts of the world (Liu et al., 2015). Our results strengthen research demonstrating that a warmer and dryer world could hamper ecosystem productivity over broad areas, with a considerable socio-economic impact and significant consequences on carbon storage (Beck et al., 2011; Piao et al., 2014). A better understanding and a more accurate simulation of the links between the environment and NDVI are currently a crucial stake to understand the effects of the global climate change on vegetation, monitor its consequences, and try to adapt our environment to future conditions.

Acknowledgements

This work was supported by the French National Research Agency through the Laboratory of Excellence ARBRE, the GIP ECOFOR and the RMT AFORCE, the Regional Council of Lorraine, and the Direction Régionale de l'Alimentation, de l'Agriculture et de la Forêt of the Lorraine region. We also thank Vanessa Drolon and Janick Moukambo for their help.

Supplementary data

Supplementary data to this article can be found online at https://doi.org/10.1016/j.scitotenv.2018.10.052.

References

Allen, C.D., et al., 2010. A global overview of drought and heat-induced tree mortality reveals emerging climate change risks for forests. For. Ecol. Manag. 259 (4), 660–684.
Beck, P.S.A., et al., 2011. Changes in forest productivity across Alaska consistent with biome shift. Ecol. Lett. 14 (4), 373–379.
Bergès, L., Balandier, P., 2010. Revisiting the use of soil water budget assessment to predict site productivity of sessile oak (Quercus petraea Liebl.) in the perspective of climate change. Eur. J. For. Res. 129 (2), 199–208.
Beven, K.J., Kirkby, M.J., 1979. A physically based, variable contributing area model of basin hydrology/Un modèle à base physique de zone d'appel variable de l'hydrologie du bassin versant. Hydrol. Sci. Bull. 24 (1), 43–69.
Bigler, C., Braker, O.U., Bugmann, H., Dobbertin, M., Rigling, A., 2006. Drought as an inciting mortality factor in Scots pine stands of the Valais, Switzerland. Ecosystems 9 (3), 330–343.
Boisvenue, C., Running, S.W., 2006. Impacts of climate change on natural forest productivity - evidence since the middle of the 20th century. Glob. Chang. Biol. 12 (5), 862–882.
Bontemps, J.D., Herve, J.C., Leban, J.M., Dhote, J.F., 2011. Nitrogen footprint in a long-term observation of forest growth over the twentieth century. Trees-Struct. Funct. 25 (2), 237–251.
Breda, N., Huc, R., Granier, A., Dreyer, E., 2006. Temperate forest trees and stands under severe drought: a review of ecophysiological responses, adaptation processes and long-term consequences. Ann. For. Sci. 63 (6), 625–644.
Buermann, W., et al., 2014. Recent shift in Eurasian boreal forest greening response may be associated with warmer and drier summers. Geophys. Res. Lett. 41 (6), 1995–2002.
Carnicer, J., et al., 2011. Widespread crown condition decline, food web disruption, and amplified tree mortality with increased climate change-type drought. Proc. Natl. Acad. Sci. U. S. A. 108 (4), 1474–1478.
Charru, M., Seynave, I., Hervé, J.C., Bontemps, J.D., 2014. Spatial patterns of historical growth changes in Norway spruce across western European mountains and the key effect of climate warming. Trees-Struct. Funct. 28 (1), 205–221.
Charru, M., Seynave, I., Herve, J.C., Bertrand, R., Bontemps, J.D., 2017. Recent growth changes in Western European forests are driven by climate warming and structured across tree species climatic habitats. Ann. For. Sci. 74 (2), 1–34.
Chen, T., de Jeu, R.A.M., Liu, Y.Y., van der Werf, G.R., Dolman, A.J., 2014. Using satellite based soil moisture to quantify the water driven variability in NDVI: a case study over mainland Australia. Remote Sens. Environ. 140, 330–338.
Chéret, V., Denux, J.P., 2007. Mapping wildfire danger at regional scale with an index model integrating coarse spatial resolution remote sensing data. J. Geophys. Res. Biogeosci. 112 (G2).
Chéret, V., Denux, J.P., 2011. Analysis of MODIS NDVI time series to calculate indicators of Mediterranean forest fire susceptibility. Gisci. Remote Sensing 48 (2), 171–194.
Djebou, D.C.S., Singh, V.P., Frauenfeld, O.W., 2015. Vegetation response to precipitation across the aridity gradient of the southwestern United States. J. Arid Environ. 115, 35–43.
Dorman, M., Svoray, T., Perevolotsky, A., 2013. Homogenization in forest performance across an environmental gradient - the interplay between rainfall and topographic aspect. For. Ecol. Manag. 310, 256–266.
Dyer, J.M., 2009. Assessing topographic patterns in moisture use and stress using a water balance approach. Landsc. Ecol. 24 (3), 391–403.
Fensholt, R., et al., 2012. Greenness in semi-arid areas across the globe 1981–2007 - an Earth Observing Satellite based analysis of trends and drivers. Remote Sens. Environ. 121, 144–158.
Forkel, M., et al., 2015. Codominant water control on global interannual variability and trends in land surface phenology and greenness. Glob. Chang. Biol. 21 (9), 3414–3435.
Fotheringham, A.S., Brunsdon, C., Charlton, M.E., 2002. Geographically Weighted Regression: The Analysis of Spatially Varying Relationships. Wiley, Chichester, UK (284 pp.).
Gegout, J.C., Herve, J.C., Houllier, F., Pierrat, J.C., 2003. Prediction of forest soil nutrient status using vegetation. J. Veg. Sci. 14 (1), 55–62.
Gibelin, A., et al., 2014. Évolution de la température en France depuis les années 1950. Constitution d'un nouveau jeu de séries homogénéisées de référence. La Météorologie 87, 45–53.
Gordo, O., Sanz, J.J., 2010. Impact of climate change on plant phenology in Mediterranean ecosystems. Glob. Chang. Biol. 16 (3), 1082–1106.
Granier, A., Breda, N., Biron, P., Villette, S., 1999. A lumped water balance model to evaluate duration and intensity of drought constraints in forest stands. Ecol. Model. 116 (2–3), 269–283.
Gromping, U., 2006. Relative importance for linear regression in R: the package relaimpo. J. Stat. Softw. 17 (1).
Guo, L., et al., 2014. NDVI-based vegetation change in inner Mongolia from 1982 to 2006 and its relationship to climate at the biome scale. Adv. Meteorol. 4, 1–12.
Hew, C.S., Krotkov, G., Canvin, D.T., 1969. Effects of temperature on photosynthesis and CO_2 evolution in light and darkness by green leaves. Plant Physiol. 44 (5), 671–677.
Huete, A., et al., 2002. Overview of the radiometric and biophysical performance of the MODIS vegetation indices. Remote Sens. Environ. 83 (1–2), 195–213.
Hui, S., Mo, X.G., Lin, Z.H., 2014. Optimizing the photosynthetic parameter V-cmax by assimilating MODIS-f(PAR) and MODIS-NDVI with a process-based ecosystem model. Agric. For. Meteorol. 198, 320–334.
IPCC, S., T.F., Qin, D., Plattner, G.-K., Tignor, M., Allen, S.K., Boschung, J., Nauels, A., Xia, Y., Bex, V., Midgley, P.M., 2013. IPCC, 2013: Climate Change 2013: The Physical Science Basis. Contribution of Working Group I to the Fifth Assessment Report of the Intergovernmental (eds.), Cambridge, United Kingdom and New York, NY, USA.
Jeong, G., et al., 2017. Environmental drivers of spatial patterns of topsoil nitrogen and phosphorus under monsoon conditions in a complex terrain of South Korea. PLoS One 12 (8).
Jin, J.X., et al., 2014. Climate change contribution to forest growth in eastern China over past two decades. Terr. Atmos. Ocean. Sci. 25 (1), 49–60.
Jönsson, Per, Eklundh, Lars, 2004. TIMESAT—a program for analyzing time-series of satellite sensor data. Comput. Geosci. 30 (8), 833–845.
Julien, Y., Sobrino, J.A., Verhoef, W., 2006. Changes in land surface temperatures and NDVI values over Europe between 1982 and 1999. Remote Sens. Environ. 103 (1), 43–55.
Kawabata, A., Ichii, K., Yamaguchi, Y., 2001. Global monitoring of interannual changes in vegetation activities using NDVI and its relationships to temperature and precipitation. Int. J. Remote Sens. 22 (7), 1377–1382.
Kogan, F., Gitelson, A., Zakarin, E., Spivak, L., Lebed, L., 2003. AVHRR-based spectral vegetation index for quantitative assessment of vegetation state and productivity: calibration and validation. Photogramm. Eng. Remote Sens. 69 (8), 899–906.
Lenoir, J., Gégout, J.C., Marquet, P.A., de Ruffray, P., Brisse, H., 2008. A significant upward shift in plant species optimum elevation during the 20th century. Science 320 (5884), 1768–1771.
Lindeman, R., Merenda, P., Gold, R., 1980. Introduction to Bivariate and Multivariate Analysis (444 pp.).
Liu, Y., Li, Y., Li, S.C., Motesharrei, S., 2015. Spatial and temporal patterns of global NDVI trends: correlations with climate and human factors. Remote Sens. 7 (10), 13233–13250.
Luo, H.X., et al., 2016. NDVI, temperature and precipitation variables and their relationships in Hainan Island from 2001 to 2014 based on MODIS NDVI. In: Bian, F., Xie, Y. (Eds.), Geo-informatics in Resource Management and Sustainable Ecosystem. Communications in Computer and Information Science. Springer-Verlag, Berlin, Berlin, pp. 336–344.
Meng, M., Ni, J., Zong, M., 2011. Impacts of changes in climate variability on regional vegetation in China: NDVI-based analysis from 1982 to 2000. Ecol. Res. 26 (2), 421–428.
Nestola, E., et al., 2018. Are optical indices good proxies of seasonal changes in carbon fluxes and stress-related physiological status in a beech forest? Sci. Total Environ. 612, 1030–1041.

Peled, E., Dutra, E., Viterbo, P., Angert, A., 2010. Technical note: comparing and ranking soil drought indices performance over Europe, through remote-sensing of vegetation. Hydrol. Earth Syst. Sci. 14 (2), 271–277.
Pettorelli, N., Vik, J.O., Mysterud, A., Gaillard, J.M., Tucker, C.J., Stenseth, N.C., 2005. Using the satellite-derived NDVI to assess ecological responses to environmental change. Trends Ecol. Evol. 20 (9), 503–510.
Piao, S.L., et al., 2011. Altitude and temperature dependence of change in the spring vegetation green-up date from 1982 to 2006 in the Qinghai-Xizang Plateau. Agric. For. Meteorol. 151 (12), 1599–1608.
Piao, S.L., et al., 2014. Evidence for a weakening relationship between interannual temperature variability and northern vegetation activity. Nat. Commun. 5, 5018.
Piedallu, C., Gégout, J.C., 2007. Multiscale computation of solar radiation for predictive vegetation modelling. Ann. For. Sci. 64 (8), 899–909.
Piedallu, C., Gégout, J.C., Bruand, A., Seynave, I., 2011. Mapping soil water holding capacity over large areas to predict potential production of forest stands. Geoderma 160 (3–4), 355–366.
Piedallu, C., Gégout, J.C., Perez, V., Lebourgeois, F., 2013. Soil water balance performs better than climatic water variables in tree species distribution modelling. Glob. Ecol. Biogeogr. 22, 470–482.
Piedallu, C., Gegout, J.C., Lebourgeois, F., Seynave, I., 2016. Soil aeration, water deficit, nitrogen availability, acidity and temperature all contribute to shaping tree species distribution in temperate forests. J. Veg. Sci. 27 (2), 387–399.
Quetin, G.R., Swann, A.L.S., 2017. Empirically derived sensitivity of vegetation to climate across global gradients of temperature and precipitation. J. Clim. 30 (15), 5835–5849.
Rameau, J.C., Mansion, D., Dumé, G., 1989. Flore forestièreFrançaise – guide écologique illustré – tome 1: plaines et collines. Institut pour le Développement, Paris.
Rameau, J.C., Mansion, D., Dumé, G., G., C., 2008. Flore forestière française - guide écologique illustré - tome 3: région méditerranéenne. Institut pour le Développement, Paris (2426 pp.).
Reed, B.C., Brown, J.F., VanderZee, D., Loveland, T.R., Merchant, J.W., Ohlen, D.O., 1994. Measuring phenological variability from satellite imagery. J. Veg. Sci. 5, 703–714.
Reichstein, M., et al., 2007. Reduction of ecosystem productivity and respiration during the European summer 2003 climate anomaly: a joint flux tower, remote sensing and modelling analysis. Glob. Chang. Biol. 13 (3), 634–651.
Rhee, J., Im, J., 2017. Meteorological drought forecasting for ungauged areas based on machine learning: using long-range climate forecast and remote sensing data. Agric. For. Meteorol. 237, 105–122.
Rouse, J.H.R., Schell, J., Deering, D., 1973. Monitoring vegetation systems in the great plains with ERTS. Third ERTS Symposium 1973, NASA, SP-351 I, pp. 309–317.
Scharnweber, T., et al., 2011. Drought matters - declining precipitation influences growth of *Fagus sylvatica* L. and *Quercus robur* L. in north-eastern Germany. For. Ecol. Manag. 262 (6), 947–961.
Seynave, I., et al., 2005. Picea abies site index prediction by environmental factors and understorey vegetation: a two-scale approach based on survey databases. Can. J. For. Res. 35 (7), 1669–1678.
Seynave, I., Gegout, J.C., Herve, J.C., Dhote, J.F., 2008. Is the spatial distribution of European beech (*Fagus sylvatica* L.) limited by its potential height growth? J. Biogeogr. 35 (10), 1851–1862.
Slayback, D.A., Pinzon, J.E., Los, S.O., Tucker, C.J., 2003. Northern hemisphere photosynthetic trends 1982–99. Glob. Chang. Biol. 9 (1), 1–15.
Stangler, D.F., Hamann, A., Kahle, H.P., Spiecker, H., 2017. A heat wave during leaf expansion severely reduces productivity and modifies seasonal growth patterns in a northern hardwood forest. Tree Physiol. 37 (1), 47–59.
Stephenson, N.L., 1990. Climatic control of vegetation distribution: the role of the water balance. Am. Nat. 135, 649–670.
Stephenson, N.L., 1998. Actual evapotranspiration and deficit: biologically meaningful correlates of vegetation distribution across spatial scales. J. Biogeogr. 25, 855–870.
Thornthwaite, C.W., Mather, J.R., 1955. The water balance. Publications in climatology VIII. Drexel Institute of Climatology Laboratory, Centerton, NJ, pp. 1–104.
Tucker, C.J., Townshend, J.R.G., Goff, T.E., 1985. African land-cover classification using satellite data. Science 227 (4685), 369–375.
Turc, L., 1961. Evaluation des besoins en eau d'irrigation et évaporation potentielle. Ann. Agron. 12, 13–49.
Vallet, P., Perot, T., 2016. Tree diversity effect on dominant height in temperate forest. For. Ecol. Manag. 381, 106–114.
Vennetier, M., Ripert, C., 2009. Forest flora turnover with climate change in the Mediterranean region: a case study in Southeastern France. For. Ecol. Manag. 258, S56–S63.
Verbyla, D., 2008. The greening and browning of Alaska based on 1982–2003 satellite data. Glob. Ecol. Biogeogr. 17 (4), 547–555.
Vicente-Serrano, S.M., et al., 2013. Response of vegetation to drought time-scales across global land biomes. Proc. Natl. Acad. Sci. U. S. A. 110 (1), 52–57.
Walker, D.A., et al., 2003. Phytomass, LAI, and NDVI in northern Alaska: relationships to summer warmth, soil pH, plant functional types, and extrapolation to the circumpolar Arctic. J. Geophys. Res.-Atmos. 108 (D2).
Wang, J., Rich, P.M., Price, K.P., 2003. Temporal responses of NDVI to precipitation and temperature in the central Great Plains, USA. Int. J. Remote Sens. 24 (11), 2345–2364.
Yao, J.Q., et al., 2018. Response of vegetation NDVI to climatic extremes in the arid region of Central Asia: a case study in Xinjiang, China. Theor. Appl. Climatol. 131 (3–4), 1503–1515.
Zewdie, W., Csaplovics, E., Inostroza, L., 2017. Monitoring ecosystem dynamics in northwestern Ethiopia using NDVI and climate variables to assess long term trends in dryland vegetation variability. Appl. Geogr. 79, 167–178.
Zhou, J.H., et al., 2016. Alpine vegetation phenology dynamic over 16 years and its covariation with climate in a semi-arid region of China. Sci. Total Environ. 572, 119–128.
Zubillaga, M., Urricariet, S., 2005. Assessment of nitrogen status in wheat using aerial photography. Commun. Soil Sci. Plant Anal. 36 (13–14), 1787–1798.